Supporting Information

Fluorescent protein display on cellular mimic enables rapid and accurate identification of natural killer cell phenotypes

Hu Liu,[a,b] Ziming Li,[a] Shanghan Zhou,[a] Jiali Chen,[a] Meiling Liu,[a] Hong-Hui Wang,[c] Youyu Zhang,[a] Ruijie Deng[b] and Xiaohua Zhu,*[a,c]

[a] Key Laboratory of Chemical Biology and Traditional Chinese Medicine Research (Ministry of Education), College of Chemistry and Chemical Engineering, Hunan Normal University, Changsha 410081, China. E-mail: zhuxiaohua@hunnu.edu.cn

[b] College of Biomass Science and Engineering, Sichuan University, Chengdu 610065, China

[c] State Key Laboratory of Chemo/Bio-Sensing and Chemometrics, College of Biology, College of Chemistry and Chemical Engineering, Hunan University, Changsha 410082, China

This content includes:

Experimental section

Reagents and materials

Dopamine hydrochloride and ethanol were purchased from Sinopharm Chemical Reagent Company (Shanghai, China). IL-2 was purchased from Sigma-Aldrich (Shanghai, China). All reagents were of analytical grade, and all solutions were prepared with ultrapure water (18.25 MΩ·cm).

Preparation of the three FPs

The amino acid sequences of BFPs, GFPs, and RFPs were referred to previous work.[1-3] The gene sequences of BFPs, GFPs, and RFPs were codon-optimized and synthesized by Sangon Biotech (Shanghai, China), and then cloned into the plasmid pUC57. PCR amplified the genes of BFPs, GFPs, and RFPs and then inserted them into the plasmid pET28a using restriction enzyme cutting sites of NdeI and EcoRI. The reconstructed plasmid pET28a-BFP, pET28a-GFP, and pET28-RFP were transformed into *E. coli* BL21 (DE3) by heat shock. Cells were grown in Luria-Bertani (LB) medium at 37 °C until the OD_{600} nm reached 0.8. After that, isopropyl β-D-1-thiogalactopyranoside was added to induce the protein expression. After being harvested by centrifugation, the cells were transferred to a lysis buffer and lysed by sonication. The proteins were purified by Ni-NTA agarose chromatography (ÄKTA, GE) and then exchanged into desalination buffer (10 mM Tris, 100 mM NaCl, 50% glycerin, pH 7.4) by desalination chromatography (ÄKTA, GE). The purified proteins were quantified by Bradford protein assay, and then were stored at -80 ºC before use.

Analysis of the theoretical net charge of the three FPs

The charge of FPs could be expressed by equation (Eq 1):

$$\text{theoretical charge} = \alpha \cdot m + \beta n - \varepsilon x - \zeta y + \theta z \qquad \text{(Eq. 1)}$$

m, n, x, y and z denote the number of Lys, Arg, Asp, Glu, and His, respectively. α, β, θ denote the protonation degree of the side chain in Lys, Arg, and His (basic amino

acid residue), respectively. At the same time, ε and ζ denote the deprotonation degree of the side chain in Asp and Glu (acidic amino acid residue), respectively.

The relationship between pH and pKa was demonstrated in the Henderson-Hasselbalch equation (Eq. 2).

$$pH = pKa + \log([A^-]/[HA]) \qquad \text{(Eq. 2)}$$

$[A^-]$ and [HA]denote the deprotonated and the protonated amino acid residues, respectively. pKa denotes the pKa value of the side chain (R) in an amino acid. The protonation degree of basic amino acids was expressed by equation (Eq. 3):

$$\text{protonation degree} = [HA]/([HA] + [A-]) \qquad \text{(Eq. 3a)}$$

$$\text{protonation degree} = 1/[1 + 10(pH - pKa)] \qquad \text{(Eq. 3b)}$$

Substitute the reported pKa value into equation (Eq. 3b). The calculated results showed that one Lys (R: -NH2, pKa = 10.54) or Arg residue (R: -CN3H4, pKa = 12.48) represents nearly one positive charge due to nearly 100% protonation of Lys or Arg at pH 5.0-7.4. The deprotonation degree of acidic amino acids was expressed by equation (Eq. 4):

$$\text{deprotonation degree} = [A-]/([HA] + [A-]) \qquad \text{(Eq. 4a)}$$

$$\text{deprotonation degree} = 1/[1 + 10(pKa - pH)] \qquad \text{(Eq. 4b)}$$

Substitute the reported pKa value into equation (Eq. 4b), the calculated result showed that one Asp (R: $-CH_2COOH$, pKa = 3.86) or Glu (R: $-CH_2CH_2COOH$, pKa = 4.25) residue represent approximately one negative charge for each amino acid, which was attributed to almost 100% deprotonation of Asp or Glu at pH 5.0-7.4.

$$\text{theoretical net charge} = m + n - x - y + z/[1 + 10(pH - pKa)] \qquad \text{(Eq. 5)}$$

pKa donates the pKa value (6.04) of the imidazole side chain in His.

Preparation of PDA

The PDA was prepared in a water−ethanol mixed solution (5:1). Briefly, 50 mL of Tris buffer solution (10 mM, pH 8.5) was mixed with 10 mL of alcohol. Then, 25 mg of dopamine hydrochloride was added to the mixed solution. The solution was stirred for 16 h at room temperature. After the reaction, the PDA was collected by centrifugation and washed with ultrapure water three times.

RBCM extraction

The vesicles derived from RBCM were prepared by differential centrifugation. The fresh whole blood from rat samples was centrifuged at 3000 rpm for 5 min to remove the plasma. The red blood cells were washed with saline three times and then hemolyzed in water at 4 ^{o}C for 1 h. Then, the RBCM was spun down at 12,000 rpm for 10 min and washed with water six times until the supernatant became colorless. Then the pellet was collected, redispersed in water, and stored at -80 ^{o}C. The works were approved by the Scientific Ethics Committee of Hunan Normal University (Project LSK-2022-166). The animal experiments were performed in compliance with the relevant laws and guidelines issued by the Ethical Committee of Hunan Normal University and were in agreement with the guidelines of the Institutional Animal Care and Use Committee.

Preparation of the PDA@EM

To 100 μL of RBCM (5 mg mL^{-1}), 400 μL of water was added. Then the pH value of the solution was adjusted to 7.4 using a diluted NaOH solution. After that, the solution was sonicated for 30 s before being mixed with 500 μL of PDA solution (0.2 mg mL^{-1}). Subsequently, the mixture was repeatedly extruded 11 times through a 220 nm polycarbonate porous membrane using a syringe filter, and then the excess RBCM was removed by centrifugation (10,000 rpm, 10 min at 4 °C). The PDA@RBCM were redispersed in PBS and stored at -80 ^{o}C for future use.

Fluorescence titration experiments

The three FP solutions were diluted using PBS (1×, pH = 7.4). Then, different concentrations of PDA@RBCM were gradually added to the FPs solution. The fluorescence intensity of the PDA@RBCM/FPs mixture was recorded with a fluorescence spectrophotometer (F7100, Japan) at excitation wavelengths of 403 nm, 480 nm, and 570 nm for BFP, GFP, and RFP, respectively.

Calculation of the binding constant between PDA@RBCM and FPs

We estimated the binding constant using the Stern-Volmer equation.[4]

$$F_0/F = 1+ Ksv[M]$$

where F_0 and F represent the fluorescence emission intensity of FPs and PDA@EM/FPs at the optimal emission wavelength. Ksv is a constant, and M is the

concentration of PDA@RBCM.

Cell culture

Chinese Hamster Ovary (CHO) cells were cultured in RPMI1640 (Procell, Wuhan, China) with 10% fetal bovine serum (Sbjbio Life Sciences, Nanjing, China) and 1% penicillin and streptomycin (NCM Biotech, Suzhou, China). Human cervical cancer (HeLa) cells and human breast cancer (MCF-7) cells were cultured in 10% v/v fetal Bovine serum (Gibco) and 1% penicillin/streptomycin in cell culture medium DMEM (Dulbecco's modified Eagle's medium, Hyclone). NK cells were seeded into 96-well plates containing 300 μL of RPMI 1640 with 10% FBS (Sbjbio Life Sciences, Nanjing, China) and incubated with different concentrations of IL-2 at 37 °C. All cells were grown at 37 °C in a humidified environment with 5% CO_2.

Array-based sensing studies

In a 96-well plate, the three FPs were diluted to 50 μL with PBS (1×, pH 7.4). The FPs were used at final concentrations of 25 nM for BFP, 20 nM for GFP, and 50 nM for RFP. PDA@RBCM (~12 μg mL^{-1}) was then added, reducing the final fluorescence intensity of the FPs by approximately 30%. After thorough mixing, the sensor array

was diluted with PBS (1×, pH 7.4) to a final volume of 90 μL. Different cell lines were subsequently introduced to achieve a final well volume of 100 μL. The samples were incubated for 15 min at 37 °C, and fluorescence intensity was measured using a Biotek microplate reader (SynergyMX, USA) across three emission channels. The excitation and emission wavelengths were 403/466 nm, 480/515 nm, and 570/616 nm for BFP, GFP, and RFP, respectively.

Linear discriminant analysis (LDA) analysis

The raw fluorescence response matrix was processed by classical LDA in Anaconda Prompt. In LDA, all variables were used in the model (complete mode) and the tolerance was set as 0.001. The raw fluorescence response patterns were transformed to canonical patterns where the ratio of between-class variance to the within-class variance was maximized according to the preassigned grouping. To identify the unknown samples, the fluorescence response patterns of the new cases were first converted to canonical scores using the discriminant functions established on the training cases. Then, the Mahalanobis distance, the distance of a case from the centroid of a training group in the multidimensional discriminant space, was calculated for the new cases. The new case was assigned to the group with the shortest Mahalanobis distance from the case.[5,6]

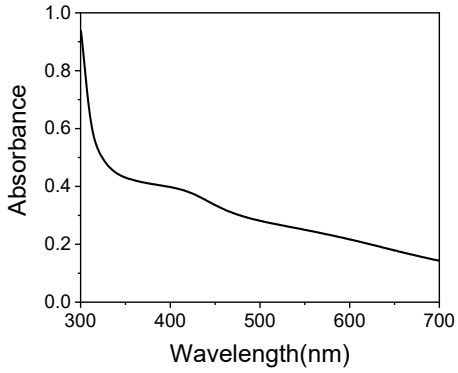

Fig. S1. UV-vis spectra of PDA.

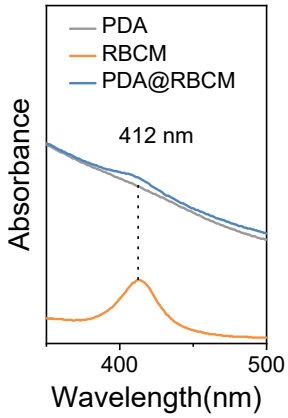

Fig. S2. UV-vis spectra of PDA, RBCM, and PDA@RBCM.

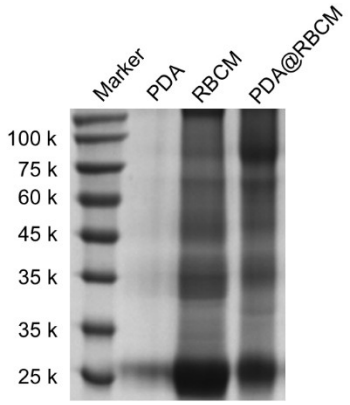

Fig. S3. SDS-PAGE and Coomassie Brilliant Blue staining of protein analysis of PDA, RBCM, and PDA@RBCM.

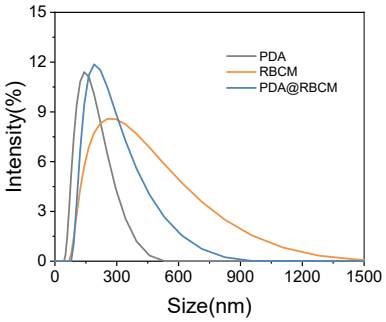

Fig. S4. The hydrodynamic diameters of PDA, RBCM, and PDA@RBCM in PBS (pH =7.4).

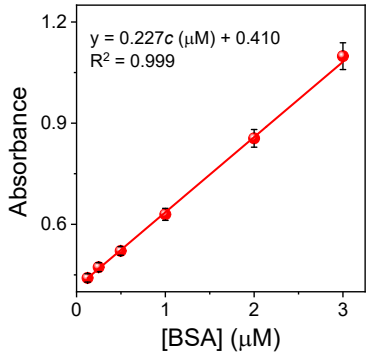

Fig. S5. Standard curve for protein determination using the BCA assay. Standard curve for the determination of protein content with varying concentrations of BSA (0 to 3 μM). The absorbance at 562 nm is plotted against the BSA concentration.

A **BFP**

MSEELIKENMHMKLYMEGTVDNHHFKCTSEGEGKPYEGTQT
MRIKVVEGGPLPFAFDILATSFLYGSKTFINHTOGIPDFFKOSFPE
GFTWERVTTYEDGGVLTATODTSLQDGCLIYNVKIRGVNFTSN
GPVMQKKTLGWEAFTETLYPADGGLEGRNDMALKLVGGSHLI
ANIKTTYRSKKPAKNLKMPGVYYVDYRLERIKEANNETYVEQHE
VAVARYCDIPSKLGHKLNLE

GFP

SKGERLFRGKVPILVELKGDVNGHKFSVRGKGKGDATRGKLTLK
FICTTGKLPVPWPTLVTTLTYGVQCFSRYPKHMKRHDFFKSAM
PKGYVQERTISFKKDGKYKTRAEVKFEGRTLVNRIKLKGRDFKEK
GNILGHKLRYNFNSHKVYITADKRKNGIKAKFKIRHNVKDGSVQ
LADHYQQNTPIGRGPVLLPRNHYLSTRSKISKDPKEKRDHMVL
LEFVTAAGIKHGRDERYK

RFP

MEEDNMAIIKEFMRFKVHMEGSVNGHEFEIEGEGEGHPYEGT
QTAKLKVTKGGPLPFAWDILSPQFMYGSKAYVKHPADIPDYLKL
SFPEGFTWERVMNFEDGGVVTVTQDSSLQDGQFIYKVKLLGI
NFPSDGPVMQKKTMGWEASTERMYPEDGALKGEINQRLKLK
DGGHYDAEVKTTYKAKKPVQLPGAYNVDIKLDITSHNEDYTIVE
OYERAEARHST

B

Protein	BFP	GFP	RFP
Total charge	-2.7	36.4	-9.7

Fig. S6. (A) Protein sequences and (B) charge calculation results of BFPs, FPs, and RFPs at pH 7.4.

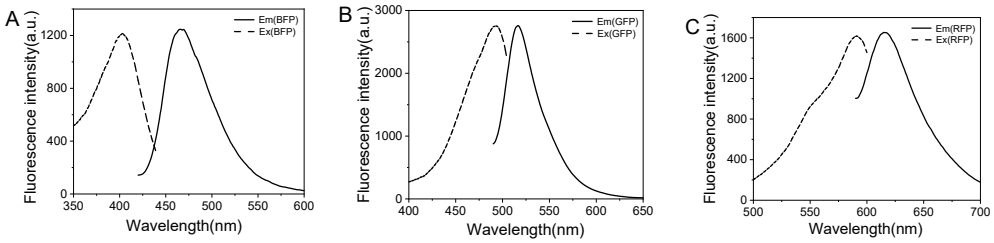

Fig. S7. The excitation and emission spectra of BFP (A), GFP (B), and RFP (C).

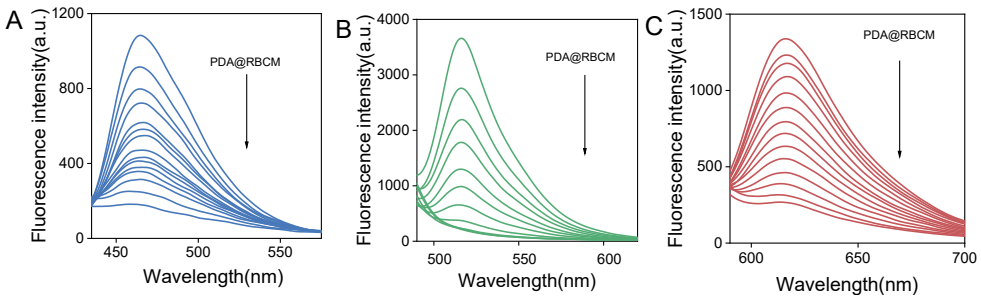

Fig. S8. (A) Fluorescence responses of BFP (200 nM) in aqueous solution upon addition of various concentrations of PDA@RBCM. (B) Fluorescence responses of GFP (50 nM) in aqueous solution upon addition of different concentrations of PDA@RBCM. (C) Fluorescence responses of RFP (200 nM) in aqueous solution upon addition of various concentrations of PDA@RBCM.

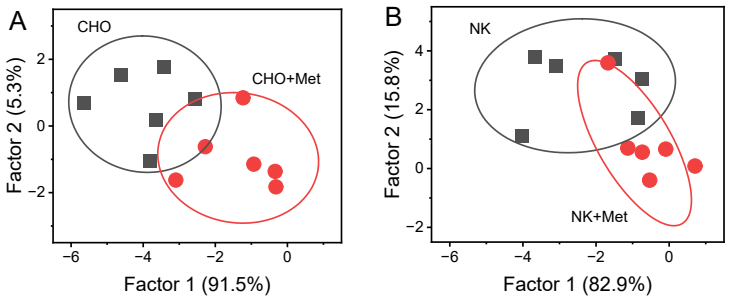

Fig. S9. LDA plot for the discrimination of CHO and CHO+Met cells with the fluorescence responses from the three FPs was quenched to ~20% (A) and 40% (B) by PDA@RBCM.

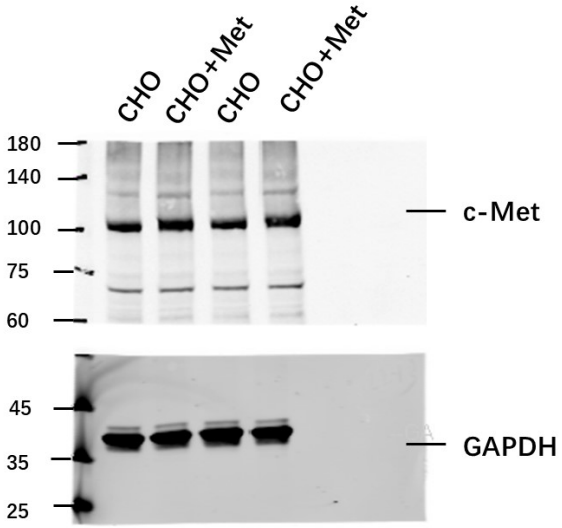

Fig. S10. Western blot analysis validating the overexpression of c-Met receptor in transfected CHO cells (CHO+Met).

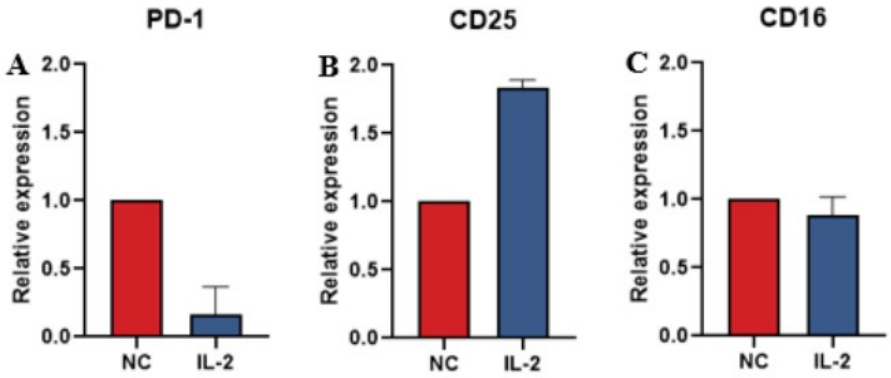

Fig. S11. RT-qPCR analysis of changes in surface proteins (A) PD-1, (B) CD25, and (C) CD16 on NK cells before and after IL-2 activation.

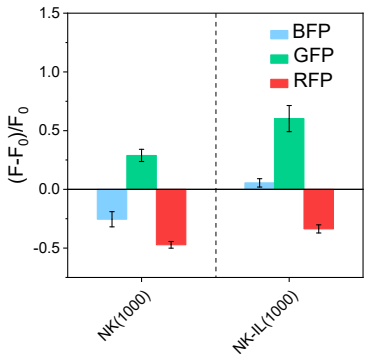

Fig. S12. Fluorescence response of NK cells and NK+IL-2.

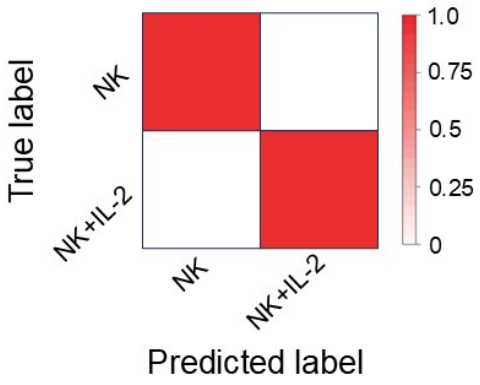

Fig. S13. Confusion matrix for NK cells identification by sensor array.

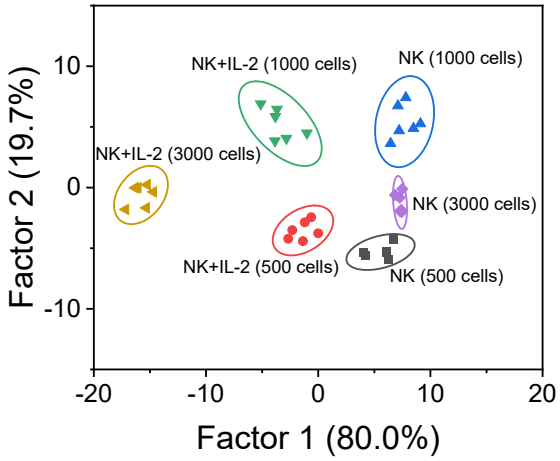

Fig. S14. LDA plot showing differentiation among varying numbers of NK cells and NK+IL-2 cells.

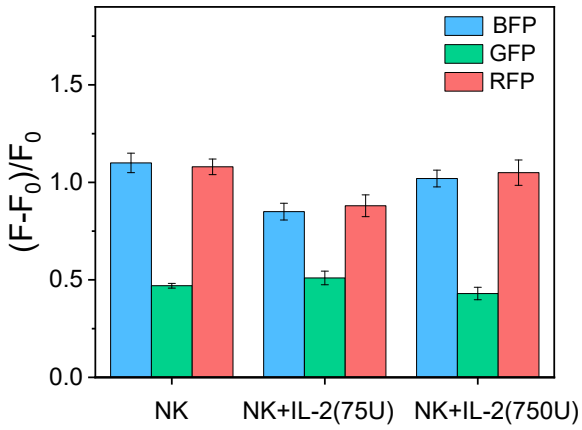

Fig. S15. Fluorescence response of NK cells, NK+IL-2 (75U), and NK+IL-2 (750U).

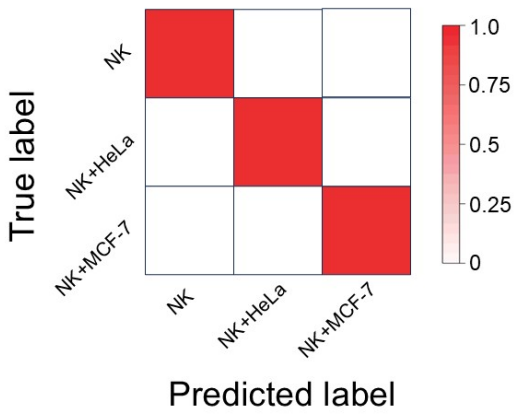

Fig. S16. LDA plot showing differentiation among varying numbers of NK cells,

NK+HeLa, and NK+MCF-7 cells.

Table S1. Binding parameters for the PDA@RBCM/FPs complexes as determined by the fitting of the fluorescence titration.

Protein	Kd, M^{-1}
BFPs	6.8×10^4
GFPs	3.8×10^5
RFPs	1.8×10^4

Table S2. Training matrix of response pattern $((F-F_0)/F_0)$ obtained from the sensor array against NK and NK+IL-2 cells. LDA was carried out and resulting in factors of the canonical scores. The jackknifed classification matrix showed 100% correct classification.

Analytes	Results LDA (The first two factors)	
cells	Factor 1	Factor 2
NK	-12.9996	3.1133
NK	-13.9995	3.9659
NK	-14.4193	5.8795
NK	-15.0410	6.3873
NK	-15.7477	4.1738
NK	-15.4076	3.9142
NK+IL-2	-5.2094	5.0161
NK+IL-2	-7.5722	5.1438
NK+IL-2	-6.8018	5.0209
NK+IL-2	-5.6657	7.4033
NK+IL-2	-4.6621	8.0465
NK+IL-2	-5.7161	6.8626

Table S3. Training matrix of response pattern ($(F-F_0)/F_0$) obtained from the sensor array against NK, NK+HeLa, and NK+MCF-7 cells. LDA was carried out and resulting in factors of the canonical scores. The jackknifed classification matrix showed 100% correct classification.

Analytes	Results LDA (The first two factors)	
cells	Factor 1	Factor 2
NK	-8.7386	-1.2315
NK	-10.3525	0.8203
NK	-9.7902	0.5765
NK	-9.4647	2.3340
NK	-8.8864	-0.5893
NK	-10.0437	1.7834
NK+MCF-7	1.9026	-1.4175
NK+MCF-7	3.5752	-1.9329
NK+MCF-7	3.2803	-1.5048
NK+MCF-7	1.1145	-2.7313
NK+MCF-7	1.9678	-2.1426
NK+MCF-7	0.3945	-1.7903
NK+HeLa	6.0984	0.6222
NK+HeLa	6.4363	0.3736
NK+HeLa	8.7640	1.0286
NK+HeLa	7.7111	3.0726
NK+HeLa	8.3284	1.1578
NK+HeLa	7.7031	1.5712

Table S4. Identification of blink samples using the sensor array.

Sample	BFP	GFP	RFP	Identification	Verification
1	0.9339	0.5248	0.9203	NK-IL2 75 U/mL	NK-IL2 75 U/mL
2	0.8990	0.4671	0.9128	NK-IL2 75 U/mL	NK-IL2 75 U/mL
3	1.0829	0.4778	1.0772	NK	NK
4	1.0017	0.4161	1.0365	NK-IL2 750 U/mL	NK-IL2 750 U/mL
5	1.0777	0.5211	1.0681	NK	NK
6	0.9962	0.4664	1.0274	NK-IL2 750 U/mL	NK-IL2 750 U/mL
7	0.9024	0.5303	0.9361	NK-IL2 75 U/mL	NK-IL2 75 U/mL
8	1.0079	0.4686	1.0449	NK-IL2 750 U/mL	NK-IL2 750 U/mL
9	1.0637	0.4978	1.0548	NK-IL2 750 U/mL	NK-IL2 750 U/mL
10	1.0819	0.5470	1.0789	NK	NK
11	1.0397	0.4651	1.0706	NK	NK
12	1.0551	0.5198	1.0590	NK	NK
13	0.9363	0.5296	0.9950	NK-IL2 75 U/mL	NK-IL2 75 U/mL
14	0.9661	0.4833	0.9643	NK-IL2 75 U/mL	NK-IL2 75 U/mL
15	0.9928	0.4638	1.0523	NK-IL2 750 U/mL	NK-IL2 750 U/mL
16	1.0466	0.5389	1.1221	NK	NK
17	0.9634	0.5479	1.0324	NK-IL2 750 U/mL	NK-IL2 750 U/mL
18	1.0189	0.4177	1.0822	NK-IL2 750 U/mL	NK-IL2 750 U/mL
19	1.0952	0.5428	1.0648	NK	NK
20	1.0942	0.5064	1.1271	NK	NK
21	1.1195	0.5690	1.0856	NK	NK
22	0.9589	0.5391	0.9643	NK-IL2 75 U/mL	NK-IL2 75 U/mL
23	0.9795	0.4739	1.0573	NK-IL2 750 U/mL	NK-IL2 750 U/mL
24	1.1206	0.5250	1.1229	NK	NK
25	0.9692	0.6210	1.0341	NK-IL2 750 U/mL	NK-IL2 750 U/mL

26	0.9116	0.4504	0.9219	NK-IL2 75 U/mL	NK-IL2 75 U/mL
27	0.9603	0.4126	0.9884	NK-IL2 75 U/mL	NK-IL2 75 U/mL
28	0.9716	0.4502	0.9510	NK-IL2 75 U/mL	NK-IL2 75 U/mL
29	0.9949	0.4038	1.0515	NK-IL2 750 U/mL	NK-IL2 750 U/mL
30	0.8822	0.4794	0.9377	NK-IL2 75 U/mL	NK-IL2 75 U/mL

References

1. O. M. Subach, I. S. Gundorov, M. Yoshimura, F. V. Subach, J. Zhang, D. Grüenwald, E. A. Souslova, D. M. Chudakov and V. V. Verkhusha, *Chem. Biol.,* 2008, **15**, 1116–1124.

2. C. Lei, Y. Huang, Z. Nie, J. Hu, L. Li, G. Lu, Y. Han and S. Yao, *Angew. Chem. Int. Ed.,* 2014, **53**, 8358 –8362.

3. H. B. Nguyen, L. W. Hung, T. O. Yeates, T. C. Terwilliger and G. S. Waldo, *Acta. Crystallogr. D Biol. Crystallogr*., 2013, **69**, 2513–2523.

4. J. Gao, X. Zhu, Y. Long, M. Liu, H. Li, Y. Zhang and S. Yao, *Anal. Chem.,* 2024, **96**, 1795−1802.

5. S. Rana, A. K. Singla, A. Bajaj, S. G. Elci, O. R. Miranda, R. Mout, B, Yan, F. R. Jirik and V. M. Rotello, *ACS Nano,* 2012, **6**, 8233–8240.

6. S. Rana, N. D. B. Le, R. Mout, B. Duncan, S. G. Elci, K. Saha, and V. M. Rotello, *ACS Cent. Sci.*, 2015, *1*, 191−197.